Correlating Mechanical Strain with Low-Temperature Hydrogenation Activity on Submonolayer Ni/W(110) Surfaces

Neetha A. Khan and Jingguang G. Chen*

Center for Catalytic Science and Technology (CCST), Department of Materials Science and Engineering, University of Delaware, Newark, Delaware 19716

Received: October 28, 2002; In Final Form: February 3, 2003

In the current paper we report a unique low-temperature hydrogenation pathway on submonolayer Ni/W(110) surfaces, which does not occur on either clean W(110) or on Ni/W(110) surfaces with Ni coverages greater than one monolayer (ML). Cyclohexene (c-C_6H_{10}) is used as a probe molecule to investigate the hydrogenation activity of Ni films deposited on a W(110) surface. Using Auger electron spectroscopy (AES), temperature-programmed desorption (TPD), low-energy electron diffraction (LEED), X-ray photoelectron spectroscopy (XPS), and high-resolution electron energy loss spectroscopy (HREELS), we have studied the reaction products and the bonding mechanisms of cyclohexene on various Ni/W(110) surfaces. On a clean W(110) surface, cyclohexene molecules undergo decomposition without producing the hydrogenation product, cyclohexane (c-C_6H_{12}). In contrast, a low-temperature (237 K) hydrogenation pathway is detected after the W(110) surface is covered with submonolayer coverages of Ni. The maximum hydrogenation activity occurs at approximately 0.4 ML Ni, which corresponds to a Ni coverage regime with high values of tensile strain on the Ni/W(110) bimetallic surfaces.

1. Introduction

Bimetallic surfaces, particular those with the coverages of the admetals in the submonolayer to monolayer range, have gained considerable interest in surface science and catalysis because they possess unique physical, chemical, and electronic properties. Research in the past several years has shown that the formation of a heteronuclear metal−metal bond on the surface induces changes in the electron density for both metals.[1,2] On bimetallic surfaces, this interfacial bond has also been shown to be different than that of two metals in the bulk alloy.[3] Depending on the atomic structure of the two metals involved, the heteronuclear bond can have different effects on the surface chemistry. For instance, Koel and Peck have found that the Sn−Pt bond on the Pt(111) surface increases the selectivity of the dehydrogenation of 1,3-cyclohexadiene to benzene to 100%.[4]

Research from our group has recently shown that depositing Ni on a Pt(111) surface significantly changes the surface activity of Pt(111). For example, Ni/Pt(111) surfaces with approximately monolayer Ni coverages exhibit a unique low-temperature hydrogenation of cyclohexene that is not seen on the surfaces of either bulk Ni or Pt.[5,6] There are two possible explanations for the unique chemistry on monolayer Ni/Pt(111): (1) The electronic properties of Ni are modified by the formation of the Ni−Pt surface alloy, and (2) the monolayer Ni is mechanically "strained" due to the lattice mismatch between Ni and Pt. The correlation of mechanical strain to the chemical activities has been the subject of several experimental and theoretical investigations.[7−11] For example, recent theoretical work by Mavrikakis et al.[9] has clearly demonstrated that the chemical properties of metal overlayers can be affected by the degree of mechanical strain in the metal overlayer.

The main objective of the current study is to further understand the potential effect of mechanical strain by investigating the hydrogenation of cyclohexene on Ni/W(110) surfaces. There are several reasons for choosing the Ni/W(110) surfaces in the current study. First, W(110) and Pt(111) represent the closed-packed surfaces of the body-centered cubic (bcc) and face-centered cubic (fcc) structures, respectively; the comparison of Ni/W(110) and Ni/Pt(111) should therefore provide information about the effect of the substrate structure. Second, the Ni layer on W(110) exhibits a significant amount of tensile mechanical strain at Ni coverages up to approximately 0.4 ML Ni;[12] therefore, the Ni/W(110) surfaces offer an excellent model system for studying the effect of mechanical strain on the surface chemical activity. Third, as described briefly below, the physical properties of Ni/W(110) surfaces have been well characterized by previous studies using a variety of surface spectroscopies.

Primarily due to the interesting magnetic properties of Ni thin films on W(110), the electronic and structural properties of Ni/W(110) surfaces have been investigated using ultraviolet photoelectron spectroscopy (UPS),[13,14] X-ray photoelectron spectroscopy (XPS),[15] scanning tunneling microscopy (STM), and low-energy electron diffraction (LEED).[12,16,17] It is generally agreed that a thick Ni layer forms a distorted fcc(111) structure, due to the lattice mismatch between Ni and the W(110) structure.[12,16,17] The Ni layer exhibits a significant amount of tensile mechanical strain at coverages up to approximately 0.4 ML Ni;[12] at Ni coverages between 0.4 and 1 ML, the strain decreases as more nickel is deposited.[12] Several studies have also investigated the effect of the change in electronic structure on the adsorption and desorption of H_2 and CO.[18,19] For example, Berlowitz and Goodman have shown that hydrogen desorbs at a temperature lower than that of W(110) at Ni coverages up to ∼1.5 ML.[19]

In the current study we have used cyclohexene (c-C_6H_{10}) as a probe molecule to investigate the chemical properties of the Ni/W(110) surface at different Ni coverages. Using cyclohexene, we are able to study the hydrogenation, dehydrogenation, and

* Corresponding author. Fax: 302-831-4545. E-mail: jgchen@udel.edu.

10.1021/jp027326+ CCC: $25.00
Published on Web 04/15/2003

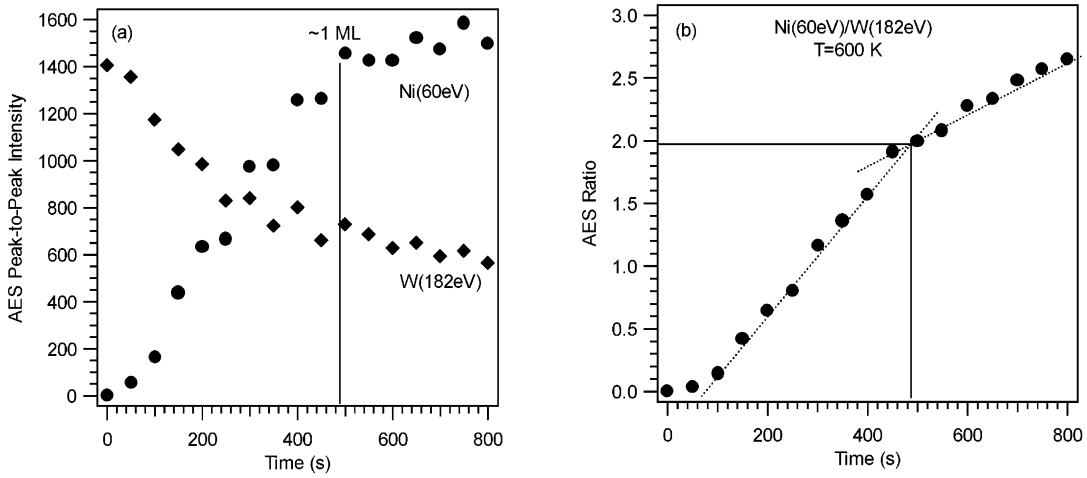

Figure 1. AES measurements following the deposition of Ni as a function of time. The left panel shows the AES intensities of Ni(60 eV) and W(182 eV) as a function of deposition time. The right-panel shows the corresponding changes in the AES intensity ratio.

decomposition pathways as a function of Ni coverage. We will show that the 0.4 ML Ni/W(110) surface has a low-temperature hydrogenation activity that is not seen on either clean W(110) or thick Ni films.

2. Experimental Section

The experiments were performed in three separate UHV systems. The TPD and AES measurements were performed in a stainless steel chamber (base pressure of 1×10^{-10} Torr) equipped with AES, LEED, and TPD, as has been described in detail previously.[6,20] For the TPD experiments, a linear heating rate of 3 K/s was used to heat the W(110) crystal in front of the mass spectrometer. The crystal was placed ~5 mm from the opening of the random flux shield of the quadrupole mass spectrometer.

The XPS measurements were taken in a separate UHV chamber, equipped with XPS, AES, and LEED. XPS spectra were taken with Al Kα radiation and a pass energy of 50 eV. The binding energy for the peaks of Ni(2p) were referenced with those of W(4f) for W(110), set at a binding energy of 31.0 eV. The cleanliness of the W(110) and Ni/W(110) surfaces was checked using AES.

Vibrational spectra were taken on a third UHV chamber equipped with HREELS, TPD, AES, and LEED. The HREELS chamber has been described in earlier publications.[21] The spectra reported here have been acquired with a primary beam energy of 6 eV using an LK-3000 HREEL Spectrometer. The spectral resolution is between 30 and 40 cm^{-1} at an elastic peak intensity between 5.0×10^4 and 2.5×10^5 cps (counts per second).

The tungsten single crystal sample was a [110] oriented, 1.5 mm thick disk (99.999%), 8 mm in diameter, and was purchased from Metal Crystals and Oxides, Ltd., Cambridge, England. The crystal was spot welded directly to two tantalum posts that serve as electrical connections for resistive heating, as well as thermal contacts for cooling with liquid nitrogen. With this mounting scheme, the temperature of the crystal could be varied between 90 and 1200 K. Cyclohexene (Aldrich, 99+% purity) was purified by successive freeze−pump−thaw cycles prior to usage and verified in-situ by mass spectrometry. Oxygen, neon, and hydrogen were all of research grade purity and were introduced into the UHV chamber without further purification. Doses are reported in langmuirs (1 langmuir = 1×10^{-6} Torr s) and are uncorrected for ion gauge sensitivities. In all experiments, cyclohexene and H_2 exposures were made at a crystal temperature of 110 K. The H_2 was on a directional dosing tube, but the cyclohexene dosings were carried out by backfilling the chamber.

A clean W(110) crystal surface is prepared by oxygen treatment at 1000 K, flash treated to 1200 K for 10 s, followed by 5 min of Ne^+ sputtering at 400 K (sample current ~5 μA) and annealing to 1200 K. Auger analysis reveals that the C and O surface impurities are both less than 1% of a monolayer after the above cleaning procedure. The nickel layer was deposited from an evaporative doser, which consisted of ultrapure Ni wire (99.999% Ni, 0.25 mm in diameter) wrapped around a resistively heated tungsten filament, mounted in a stainless steel enclosure with an opening of 1 cm in diameter. After initial conditioning, the amount of impurity (C and O) buildup was less than 5% of a monolayer. These impurities had a minor effect on the reactivity of the surfaces. During deposition, the W(110) surface was positioned approximately 2 cm from the Ni doser opening, with the surface perpendicular to the doser axis.

3. Results

3.1. Surface Characterization. There have been a number of investigations of the growth mode of Ni layers on the W(110) surface. Goodman et al. have reported pseudomorphic growth up to 1 ML at a crystal temperature of 300 K.[15,19] Other groups have observed layer-by-layer growth for up to 3 layers at 300 K.[16] For Ni coverages up to 1 ML, annealing to 790 K does not cause the clustering of the Ni overlayer. However, for Ni/W(110) surfaces with Ni coverages greater than one monolayer, annealing to 790 K induces island formation on top of one monolayer of Ni, suggesting a kinetically limited Stranski−Krastanov (SK) growth.[16] In the current study, we have used AES to estimate the Ni surface coverage ($T_{deposit}$ = 600 K) on W(110). We have chosen the deposition temperature of 600 K because it produces Ni overlayers with much less carbon contamination (<0.05 ML) than those obtained at 300 K. Figure 1 shows the AES profile of Ni(60 eV) and W(182 eV) as a function of deposition time, with the arbitrary intensity shown in Figure 1a and the Ni/W intensity ratio shown in Figure 1b. Figure 1b illustrates a change in slope when the AES ratio is about 2.0. We have used this as an indication of the onset of a monolayer. We have also attempted to use LEED to characterize the surface coverage of Ni on W(110). The transition of a (7×1) to (8×1) overlayer structure has been reported to occur at a Ni coverage of 0.4 ML by Schmidthals et al.[16,17] However, we were unable to clearly differentiate the (7×1) and (8×1)

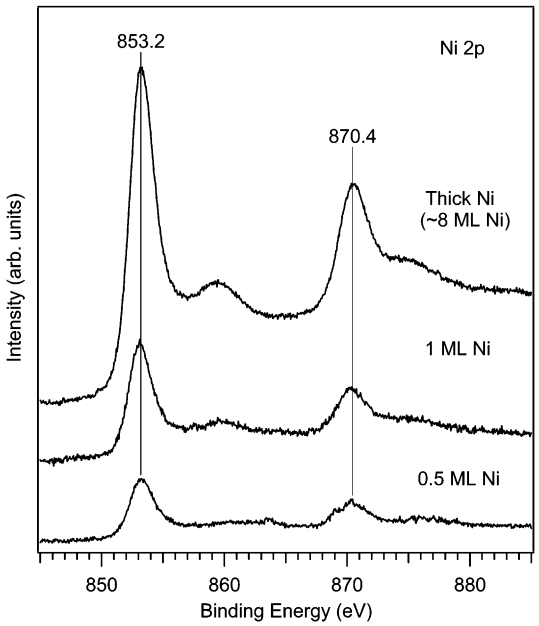

Figure 2. XPS of Ni(2p) of 0.5 ML Ni/W(110), 1 ML Ni/W(110), and thick Ni/W(110) surfaces.

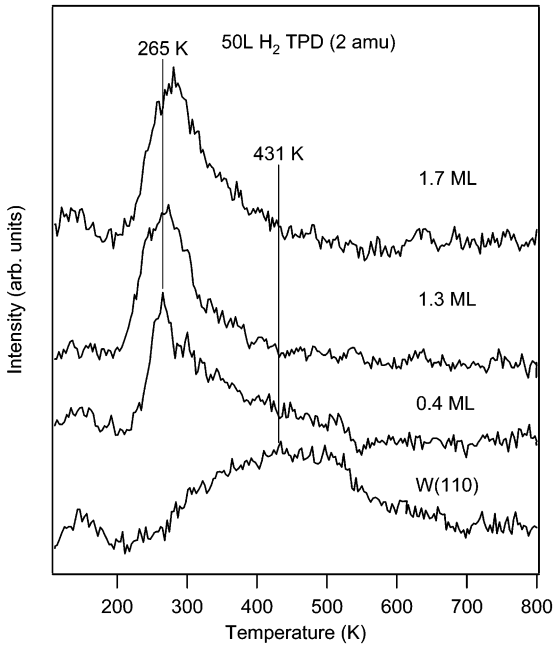

Figure 3. H_2 desorption after exposing clean W(110) and Ni/W(110) surfaces to 50 L of hydrogen. The coverage of Ni varies from 0.4 to 1.7 ML.

LEED patterns, most likely due to the limitation of image resolution in our analogue LEED system. Therefore we have based our calibration of coverage using the AES calibration curve in Figure 1b instead of using LEED.

We have also compared our Ni/W(110) surfaces with those reported by Schmidthals et al.,[16] who deposited Ni at 300 K and subsequently annealed the surfaces to 790 K for their LEED and STM characterization. For example, we conducted cyclohexene TPD experiments on two surfaces with an identical submonolayer Ni coverage: Ni deposited at 600 K and Ni deposited at 300 K, followed by annealing to 790 K. Both TPD experiments led to the same results. Therefore, we assumed that our 600 K Ni/W(110) surfaces had surface structures similar to the 790 K Ni/W(110) surfaces that were characterized by Schmidthals et al.[16]

In addition to AES experiments, XPS measurements were conducted to compare the electronic properties of the Ni/W(110) surface with Ni coverages up to 1 ML. As shown in Figure 2, the peak positions of the Ni(2p) states are identical for Ni/W(110) surfaces with 0.5, 1.0 ML, and a thicker layer of Ni, indicating that the oxidation state of Ni is similar for the submonolayer and monolayer surfaces. These results agree well with those of Goodman et al., who reported a negligible peak shift for Ni/W(110) surfaces with Ni coverages from 0.5 to 30 ML.[15]

3.2. TPD Results. *3.2.1. Reaction of Hydrogen on W(110) and Ni/W(110).* TPD experiments were carried out on Ni/W(110) surfaces with varying Ni coverages. Figure 3 shows spectra of a saturation exposure of H_2 on Ni/W(110) surfaces with different Ni coverages. In agreement with previous publications,[18,19] H_2 desorbs at 265 K from the Ni/W(110) surfaces with Ni coverages at or around 1 ML. In contrast, H_2 desorbs from the W(110) surface as a very broad peak from 300 to 550 K.[22] The low desorption temperature of H_2 on the Ni/W(110) surfaces suggests that the metal−H bond is weaker on this surface than on the W(110) surface.

The recombinative desorption temperature for H_2 should be related to the binding energy of atomic H on the surface. The adsorption and dissociation of hydrogen are considered to be unactivated on many transition metal surfaces, such as Ni.[23] Assuming this is the case for the W(110) and Ni/W(110) surfaces, the activation energy for desorption should be the same as that for the recombination of H atoms to H_2. The dissociative adsorption of H_2 can be described by the following process:

$$H_{2(g)} \rightarrow 2H_{(g)} \quad \Delta H_D$$

$$2H_{(g)} \rightarrow 2H_{(ads)} \quad 2HBE$$

where ΔH_D is the heat of dissociation and HBE is the hydrogen binding energy. The overall heat of adsorption (and desorption), ΔH_{ads}, is then

$$\Delta H_{ads} = \Delta H_D + 2HBE$$

$$HBE = 0.5\{\Delta H_{ads} - \Delta H_D\}$$

Because ΔH_D is constant, the value of HBE on different surfaces should be directly related to the ΔH_{ads}, which is related to the desorption temperature of H_2.

We have recently performed density functional theory (DFT) calculations of the values of HBE on different monometallic and bimetallic surfaces, including Ni, W, and Ni/W.[24] The DFT results indicate that the binding energy of hydrogen on Ni/W is lower than that on either Ni or W, which is in excellent agreement with the trend from the TPD measurements in Figure 1.

3.2.2. Reaction of Cyclohexene on W(110) and Ni/W(110). In our previous studies on Ni/Pt(111) with 1 ML Ni coverage, we have observed that the presence of weakly bonded $H_{(ads)}$ leads to the low-temperature hydrogenation of cyclohexene.[5] Therefore, in the current study we use the same probe reaction to determine whether the weakly adsorbed $H_{(ads)}$ on Ni/W(110) results in the low-temperature hydrogenation. Figure 4 shows the TPD spectra of H_2, benzene (C_6H_6), and cyclohexane (c-C_6H_{12}) after exposing W(110) and Ni/W(110) surfaces to 5 L of C_6H_{10} at 110 K. As shown in the left panel of Figure 4, the detection of the H_2 and benzene products on all surfaces indicates that W(110) and Ni/W(110) surfaces are active toward

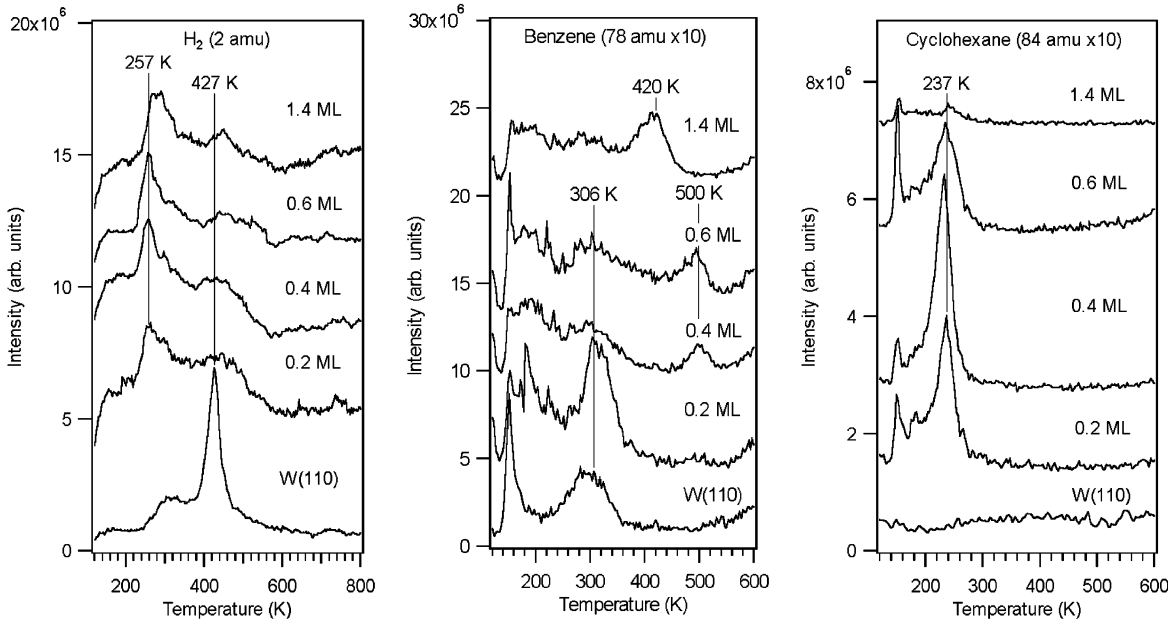

Figure 4. TPD results of the desorption of reaction products, H_2, benzene, and cyclohexane from the reaction of cyclohexene on W(110) and Ni/W(110) surfaces. The coverage of Ni varies from 0.4 to 1.4 ML.

the dissociation of cyclohexene. However, the peak areas are different on different surfaces, as will be quantified later. The more interesting observation in Figure 4 is the production of the hydrogenation product, *c*-C_6H_{12}. Although the amount of *c*-C_6H_{12} is negligible from clean W(110) or the 1.4 ML Ni/W(110) surface, the production of *c*-C_6H_{12} is clearly detected on the three Ni/W(110) surfaces with submonolayer coverages. Among them, the maximum hydrogenation activity occurs on the Ni/W(110) surface with a Ni coverage of 0.4 ML.

In addition, the peak area and desorption temperature of benzene also depend on the coverage of Ni on W(110). As shown in the middle panel in Figure 4, the desorption of the benzene product occurs from clean W(110) at 306 K. This peak remains on Ni/W(110) surfaces with Ni coverages up to 0.6 ML. This peak appears to be sharper and more intense on the 0.2 ML Ni/W(110) surface, indicating that this surface is more active toward the dehydrogenation of cyclohexene to benzene than either clean W(110) or Ni/W(110) with Ni coverages greater than 0.2 ML.

To quantify the TPD peak area of *c*-C_6H_{12}, we have performed the TPD measurements following the reversible desorption of cyclohexane from the 0.4 ML Ni/W(110) surface. In this experiment the 0.4 ML Ni/W(110) surface was exposed to 2.0 L of *c*-C_6H_{12} at 100 K. Using the standard sensitivity factors in AES, the amount of *c*-C_6H_{12} on Ni/W(110) at 100 K was estimated using AES to be 0.06 molecules/W atom. The TPD experiment was performed on another freshly prepared 2.0 L of cyclohexane on the 0.4 ML Ni/W(110) surface, as shown in Figure 5. The reversible desorption of cyclohexane was confirmed by the absence of an Auger C signal after the TPD measurement and by the absence of any reaction products (H_2, benzene, or cyclohexane) in the TPD measurement. Therefore, the TPD peak area of the 2.0 L *of* *c*-C_6H_{12} exposure in Figure 5 corresponds to a value of 0.06 cyclohexane/W atom. In comparison, this peak area is about six times that of the production of cyclohexane from the reaction of *c*-C_6H_{10} on the 0.4 ML Ni/W(110) surface (bottom spectrum in Figure 5). In addition, the comparison of the two spectra in Figure 5 also indicates that the production of cyclohexane (at 234 K) is a reaction-limited process because the reversible desorption of *c*-C_6H_{12} occurs at 191 K from the 0.4 ML Ni/W(110) surface.

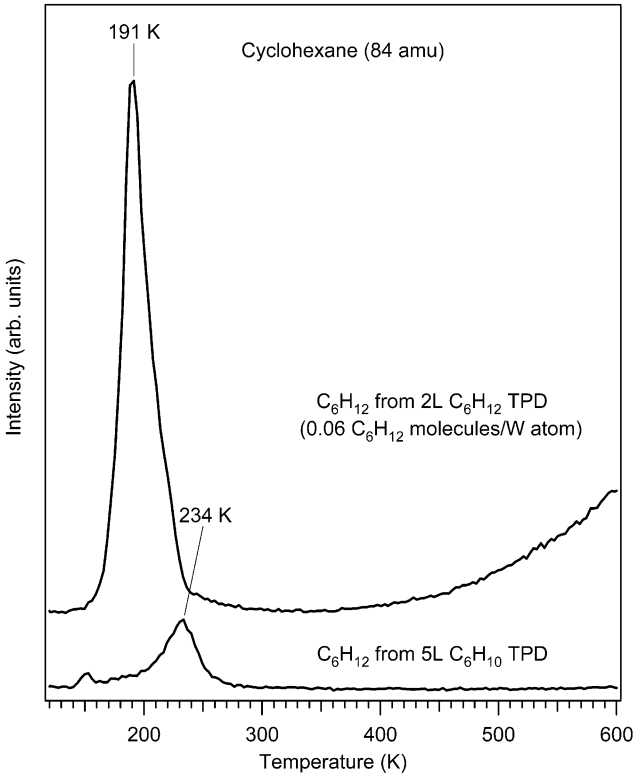

Figure 5. TPD of 84 amu from 2.0 L of *c*-C_6H_{12} from 0.4 ML Ni/W(110) and from the hydrogenation of *c*-C_6H_{10}.

3.2.3 Product Selectivity and Surface Activity. By combining the TPD results in Figure 4 with AES measurements, the product selectivity for hydrogenation, dehydrogenation, and decomposition were estimated as follows. On clean W(110), cyclohexene decomposes to atomic C and H as well as dehydrogenates to benzene, as shown in the following two equations:

$$a\mathrm{C_6H_{10}(ads)} \rightarrow 6a\mathrm{C(ads)} + 5a\mathrm{H_2(g)} \quad (1)$$

$$b\mathrm{C_6H_{10}(ads)} \rightarrow b\mathrm{C_6H_6(g)} + 2b\mathrm{H_2(g)} \quad (2)$$

The determination of surface activity and product selectivity

TABLE 1: Surface Activity and Product Selectivity of Cyclohexene on W(110) and Ni/W(110)

	activity (per W atom)				selectivity (%)		
surface	C_6H_6	C_6H_{12}	decomposition	overall	H_6	C_6H_{12}	decomposition
W(110)	0.0015		0.080	0.082	1.8		98.2
0.4 ML Ni/W(110)	0.0015	0.010	0.084	0.096	1.5	10.5	88
1.4 ML Ni/W(110)	0.0020	0.0007	0.099	0.102	2	0.7	97.3
0.5 L of H/0.4 ML Ni/W(110)		0.020					

of the clean W(110) surface was based on AES and TPD results, as discussed in detail in ref 25. Using the values reported in ref 22 for an unsaturated exposure, the values for our saturation exposures for *a* and *b* are determined to be 0.080 ± 0.009 and 0.0015 ± 0.0002 molecules per W atom, respectively. The error bars were derived from two sets of AES and TPD measurements. The temperature in this article differs slightly (within 20 K) from that in ref 25 because the experiments were done in different UHV chambers.

When Ni is present on the W(110) surface, the hydrogenation reaction pathway is present, leading to the formation of cyclohexane. The three pathways of cyclohexene hydrogenation on Ni/W(110) are shown below:

$$c\mathrm{C_6H_{10}(ads)} \rightarrow 6c\mathrm{C(ads)} + 5c\mathrm{H_2(g)} \quad (3)$$

$$d\mathrm{C_6H_{10}(ads)} \rightarrow d\mathrm{C_6H_6(g)} + 2d\mathrm{H_2(g)} \quad (4)$$

$$e\mathrm{C_6H_{10}(ads)} + e\mathrm{H_2(ads)} \rightarrow e\mathrm{C_6H_{12}(g)} \quad (5)$$

Using the values from the clean W(110) surface and the peak areas for cyclohexane determined from Figures 4 and 5, the values for *c*, *d*, and *e* were calculated in the following manner. To calculate the value for *e*, the ratio of the 84 amu TPD peak area of molecularly desorbed cyclohexane to that from the dehydrogenation of cyclohexene was determined to be 6.05 (shown in Figure 5). This leads to the following relationship:

$$\frac{\mathrm{C_6H_{12}\ on\ Ni/W(110)}}{\mathrm{C_6H_{12}\ from\ C_6H_{10}\ on\ Ni/W(110)}} = 6.05 = \frac{0.06}{e} \quad (6)$$

The value of 0.06 ± 0.006 c-C_6H_{12}/W was determined on the basis of the AES measurement at 100 K, as described earlier. Using eq 6, the activity toward c-C_6H_{12} production, value *e*, was determined to be 0.010 ± 0.001 C_6H_{12} molecules/W atom.

The value for *d* was determined by comparing the peak areas of benzene production on W(110) and Ni/W(110) surfaces, as shown in eq 7:

$$\frac{\mathrm{C_6H_6\ on\ Ni/W(110)}}{\mathrm{C_6H_6\ on\ W(110)}} = 1.03 = \frac{d}{e} \quad (7)$$

The value of *d* is then determined to be 0.0015 ± 0.0002 molecules/W atom. Furthermore, the activity toward decomposition, value *c*, can be determined on the basis of the TPD peak areas of H_2 from the clean W(110) and 0.4 ML Ni/W(110) surfaces as follows. The H_2 desorbing from the W(110) surface was from both the decomposition and the dehydrogenation of cyclohexene. On the ~0.4 ML Ni/W(110) surface, H_2 is produced from cyclohexene decomposition, but $H_{(a)}$ is also consumed in producing cyclohexane. This leads to the following relationship:

$$\frac{\mathrm{H_2\ from\ W(110)}}{\mathrm{H_2\ from\ Ni/W(110)}} = 0.97 = \frac{5a + 2b}{5c + 2d - e} \quad (8)$$

By solving this equation, the value of *c* is determined to be 0.084 ± 0.001 molecules/W atom. We also tried to estimate any errors in calculating the area from the H_2 spectra by measuring the peak areas from two temperature ranges: 150−800 K and 200−800 K. The error amounted to less than 5% in the values of *c*, *d*, and *e*. From the values of *a*, *b*, *c*, *d*, and *e*, we have estimated the overall surface activity and product selectivity on clean W(110) and 0.4 ML Ni/W(110), as summarized in Table 1. The corresponding values for the 1.4 ML Ni/W surface have been calculated in a similar manner, also summarized in Table 1.

3.2.4. Effect of Preadsorbed Hydrogen. For the hydrogenation of cyclohexene, the availability of surface hydrogen, likely from the dissociation of a fraction of cyclohexene, is a critical step for the production of cyclohexane. To confirm this, we have investigated the hydrogenation of cyclohexene on Ni/W(110) surfaces that were exposed to H_2 before the adsorption of cyclohexene. Figure 6 shows the effect of preadsorbed hydrogen on the hydrogenation of cyclohexene on the 0.4 ML Ni/W(110) surface. An exposure of submonolayer (0.5 L) H_2 increases the activity by a factor of 2. In addition, the presence of preadsorbed hydrogen also results in a state that produces c-C_6H_{12} at 199 K, lower than the desorption temperature (~234 K) without preadsorbed hydrogen. The spectra of cyclohexene (82 amu) in Figure 7 shows three states of desorption, one from the multilayer and two from the monolayer, with the multilayer desorption occurring at 153 K. The monolayer desorbs at 176 K with a shoulder at 198 K. Hydrogen also desorbs in multiple states, 261 K (surface hydrogen) and 445 K (from benzene production and cyclohexene decomposition). Therefore the preadsorption of hydrogen leads to the onset of a lower-temperature desorption state, as well as an enhancement of the overall hydrogenation activity. On the other hand, the preadsorbed hydrogen does not seem to affect the peak areas of benzene and the high-temperature H_2 state.

3.3. HREELS Results. The HREELS results following the adsorption and thermal decomposition of 3 L of cyclohexene on W(110) are shown in Figure 7. The interaction of cyclohexene with the W(110) surface was studied in detail previously[25] and is shown here only for the purpose of providing a reference to the Ni/W(110) surfaces. As described earlier,[25] the absence of vibrational modes related to the C═C double bond, such as δ(C═C) at 717 cm^{-1}, ν(C═C) at 1644 cm^{-1}, and δ-(═C−H) at 3030 cm^{-1}, indicates that cyclohexene is strongly bonded to the W(110) surface. The vibrational assignment is summarized in Table 2. The HREELS spectrum at 90 K can be assigned to either the di-σ-bonded c-C_6H_{10} or σ-bonded c-C_6H_9.[25] In addition, the peaks representing the C_6 ring (between 1000 and 1500 cm^{-1}) remain essentially intact at temperatures up to 400 K. The complete decomposition of the C_6 rings occurs after the surface is heated to 600 K to produce dehydrogenated hydrocarbon fragments, as indicated by the disappearance of the C_6 ring modes and the presence of ν(C−H) modes at 2922 and 3030 cm^{-1}.[25]

HREELS results following the same thermal treatment of 3 L cyclohexene on the 0.4 ML Ni/W(110) and 1.3 ML Ni/W(110) surfaces are compared in Figure 8. The only noticeable

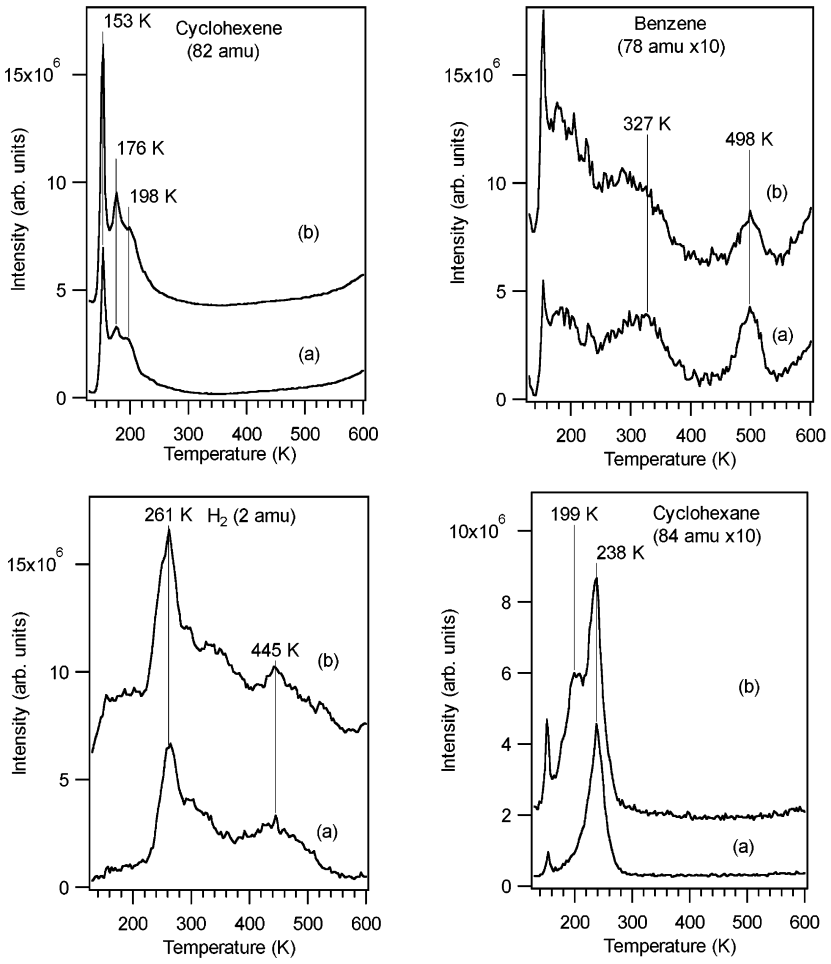

Figure 6. TPD of cyclohexene, cyclohexane, benzene, and H_2 following the reaction of cyclohexene on 0.4 ML Ni/W(110) surfaces that were preexposed to H_2 (a) 5 L of *c*-C_6H_{10}, and (b) 0.5 L of H_2/5 L of *c*-C_6H_{10}.

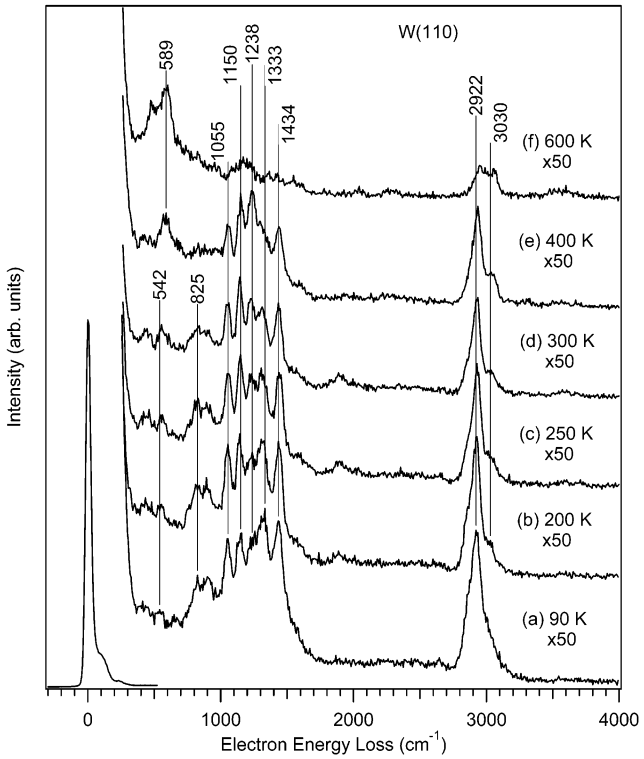

Figure 7. HREELS of 3.0 L of cyclohexene on W(110) following the adsorption at 90 K.

TABLE 2: Assignment of Vibrational Modes of 3 L of *c*-C_6H_{10} Cyclohexene Exposure on Various Surfaces

mode description	liquid	W(110)	0.4 ML Ni/W(110)	1.3 ML Ni/W(110)
ring deformation	175			
ring deformation	280			
ring deformation	393			
ring deformation	452	542	453	446
ν(metal−C)				
skeletal distortion	640, 670		649	643
δ(C═C)	720		710	731
ν(C−C)	810	825	819	798
ν(C−C)	905, 917		893	886
ν(C−C) + $\rho(CH_2)$	1038	1055	1048	1041
ωCH_2 (rock)	1138	1150	1136	1123
ωCH_2 (wag)	1241, 1264	1238	1251	1245
ωCH_2 (twist)	1321−1350	1333	1333	1326
δCH_2 (scissors)	1438−1456	1434	1441	1441
ν(C═C)	1653			
ν(−C−H)	2840−2993	2922	2922	2922
ν(═C−H)	3026−3065		3017	3017

difference between the two surfaces is detected at 90 K. As shown in the left panel of Figure 8, the 90 K spectrum on the 0.4 ML Ni/W(110) surface contains a relatively sharp C_6 skeletal distortion mode at 649 cm^{-1} and a weak ν(C═C) mode at 1630 cm^{-1}. Both features have been assigned previously as due to the presence of weakly π-bonded cyclohexene.[5] This observation indicates that, at 90 K, the interaction of cyclohexene is weaker on the 0.4 ML Ni/W(110) surface than on the 1.3 ML Ni/W(110) surface. However, after heating to 200 K, the 649

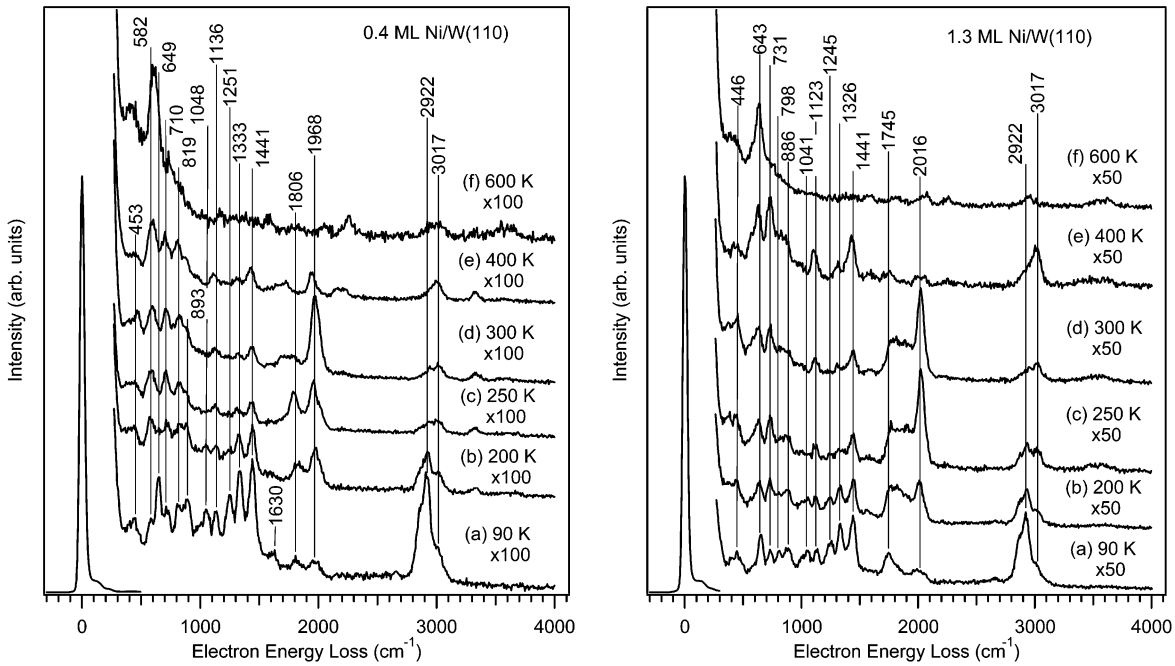

Figure 8. HREELS of 3.0 L of cyclohexene on 0.4 ML Ni/W(110) and 1.3 ML Ni/W(110) following the adsorption at 90 K. The vibrational features at 1745, 1806, 1968, and 2016 cm^{-1} are due to the adsorption of background CO during the HREELS measurements (approximately 30 min per spectrum).

and 1630 cm^{-1} features on the 0.4 ML Ni/W(110) surface disappear, leading to a near identical spectrum to its counterpart on the 1.3 ML Ni/W(110) surface.

The subsequent spectroscopic changes between 200 and 600 K are essentially identical on the two Ni/W(110) surfaces. The spectra at 200 K are representative of chemisorbed cyclohexene in a di-σ-bonded configuration, as suggested by the absence of the δ(C═C) and ν(C═C) modes. As summarized in Table 2, most of the vibrational features at 200 K can be assigned to the di-σ-bonded cyclohexene. The exception is the presence of the relatively pronounced feature at 3017 cm^{-1}, which becomes the only ν(C−H) mode at higher temperatures. As discussed in our earlier study of the reaction of cyclohexene on a thick Ni(111) film, cyclohexene underwent dehydrogenation on Ni(111) at 200 K to produce chemisorbed benzene, which was characterized by a γ(C−H) mode at ∼757−764 cm^{-1} and a ν(C−H) mode at >3000 cm^{-1}.[5] In the current study, the gradual increase in the intensities of the ν(C−H) mode at 3017 cm^{-1}, coupled with the presence of the γ(C−H) mode at 710−731 cm^{-1}, suggests that at least a fraction of cyclohexene is converted into benzene on Ni/W(110) in the temperature range of 200−400 K. Finally, decomposition begins to occur at temperatures above 200 K and all surface intermediates are completely decomposed to atomic C by 600 K; the disappearance of these features also coincides with the TPD detection of H_2 and benzene between 400 and 600 K.

4. Discussion

4.1. Hydrogenation Mechanisms on 0.4 ML Ni/W(110). As summarized in Table 1, the number of cyclohexene molecules undergoing reactions on a per W atom basis is very similar on the three surfaces: 0.080 on W(110), 0.084 on 0.4 ML Ni/W(110), and 0.099 on 1.4 ML Ni/W(110). However, the main difference is in the selectivity toward the hydrogenation product, c-C_6H_{12}, which is approximately 0% on W(110), 10.5% on 0.4 ML Ni/W(110), and 0.7% on 1.4 ML Ni/W(110). A comparison of the peak areas of c-C_6H_{12} in Figure 3 further confirms that the maximum hydrogenation activity occurs at a Ni coverage of 0.4 ML. In addition, the TPD results in Figure 6 indicate that the hydrogenation activity can be further enhanced by the preadsorption of submonolayer coverage of hydrogen on the 0.4 ML Ni/W(110) surface.

The HREELS results provide additional insights into the reaction pathways of cyclohexene on the three surfaces. After the adsorption of cyclohexene at 90 K, the ν(C═C) and δ(C═C) vibrational features are not observed on clean W(110) or 1.4 ML Ni/W(110), indicating that cyclohexene molecules interact strongly with these two surfaces at 90 K. The interaction of cyclohexene on the 0.4 ML Ni/W(110) surface is noticeably different at 90 K. The detection of the characteristic C═C vibrational modes suggests that at least a fraction of cyclohexene is weakly π-bonded on the 0.4 ML Ni/W(110) surface. However, the most important observation in Figure 8 is that the HREELS spectra on 0.4 and 1.4 ML Ni/W(110) are rather similar upon heating the surfaces to 200 K, which is below the onset temperature of c-C_6H_{12} in the TPD measurements (234 K). The HREELS results therefore suggest that the bonding of c-C_6H_{10} is similarly strong on the 0.4 ML Ni/W(110) and 1.4 ML Ni/W(110) surfaces before the production of c-C_6H_{12}.

The HREELS results on 0.4 ML Ni/W(110) are different from our previous investigation of cyclohexene on Ni/Pt(111).[5] In that study the HREEL spectrum at 200 K was indicative of weakly π-bonded cyclohexene on the monolayer Ni/Pt(111) surface.[5] We were therefore unable to conclude from that study whether the low-temperature hydrogenation of cyclohexene would require the presence of *both* weakly bonded hydrogen and weakly bonded cyclohexene on the Ni/Pt(111) surface. The results from the current study clearly indicate that the presence of weakly π-bonded cyclohexene is not a requirement for the low-temperature production of cyclohexane on the 0.4 ML Ni/W(110) surface. This in turn confirms the importance of weakly bonded hydrogen in the hydrogenation of cyclohexene.

4.2. Correlating Unique Activity on 0.4 ML Ni/W(110) with Mechanical Strain. One of the most interesting observa-

tions in the current study is that the maximum hydrogenation activity on Ni/W(110) occurs at 0.4 ML Ni, instead of at 1.0 ML Ni, as previously observed on Ni/Pt(111). One possible explanation for the maximum hydrogenation activity at 0.4 ML Ni/W(110) is the different structural properties on the surface at approximately 0.4 ML. Sander et al. have shown that, for Ni coverages below 0.4 ML, the Ni film is characterized by a tensile strain due to the lattice mismatch between the Ni overlayer and the W(110) substrate. For example, in the Ni coverage range between 0.2 and 0.4 ML, the Ni/W(110) surface was characterized by a (8×1) LEED pattern. In this configuration the tensile strain along the W[001] direction is 13% if there are 9 Ni atoms in the 8×1 unit cell (1.6% if there are 10 Ni atoms in the unit cell). However, the tensile strain disappears at Ni coverages above 0.4 ML due to the formation of a 7×1 unit cell, which leads to a compressive strain of -1.3% along the W[001] direction.[12] Additionally, these authors have used STM to demonstrate that at approximately 0.4 ML, the density of the mechanically strained (8×1) Ni island reaches a maximum on the W(110) substrate.[16] From these studies one could conclude that the overall surface tensile strain should gradually increase to a Ni coverage of 0.4 ML, and then decreases at higher Ni coverages. Therefore, the current results show a qualitative correlation between the tensile strain and the low-temperature hydrogenation of cyclohexene.

More experimental and theoretical studies are clearly needed to quantitatively understand the correlation between mechanical strain and chemical activities on Ni/W(110). Although the XPS results shown in Figure 2 indicate that the oxidation states of the 0.4 and 1.4 ML Ni/W(110) are similar, more in-depth studies of the valence electronic states, using UPS and near-edge X-ray absorption fine structure (NEXAFS)[26] will be performed soon. Such experimental measurements, coupled with theoretical calculations, such as those performed by Nørskov and coworkers on strained Ru(0001),[9] should provide a more thorough understanding of the correlation between mechanical strain, valence states, and chemical properties. The unique activity of the 0.4 ML Ni/W(110) surface and its apparent correlation with tensile strain would make Ni/W(110) an excellent model system for correlating the strain-reactivity relationship.

5. Conclusions

The combined TPD and HREELS results clearly show the presence of a low-temperature reaction pathway on submonolayer coverage Ni/W(110) surfaces, which is not present either on clean W(110) or on Ni/W(110) surfaces with coverages greater than one monolayer. Furthermore, the maximum hydrogenation activity occurs at a Ni coverage of 0.4 ML. The hydrogenation activity can be qualitatively correlated with tensile strain of the Ni/W(110) surfaces, as determined by LEED and STM by other research groups.[12,16,17] Finally, the TPD and HREELS results also suggest that the low-temperature hydrogenation on 0.4 ML Ni/W(110) is induced by the presence of weakly bonded hydrogen. However, it does not require the presence of weakly π-bonded cyclohexene prior to the hydrogenation reaction.

Acknowledgment. We thank H. Hwu for his help in acquiring the HREELS spectra. We acknowledge financial support from the Department of Energy (Grant DOE/BES DE-FG02-00ER15104). N.A.K. also acknowledges financial support from the Presidential Fellowship from the University of Delaware.

References and Notes

(1) Campbell, C. T. *Annu. Rev. Phys. Chem.* **1990**, *41*, 775.
(2) Rodriguez, J. A. *Surf. Sci. Rep.* **1996**, *24*, 225.
(3) Goodman, D. W. *J. Phys. Chem.* **1996**, *100*, 13090.
(4) Peck, J. W.; Koel, B. E. *J. Am. Chem. Soc.* **1996**, *118*, 2708.
(5) Hwu, H. H.; Eng, J.; Chen, J. G. *J. Am. Chem. Soc.* **2002**, *124*, 702.
(6) Fruhberger, B.; Eng, J.; Chen, J. G. *Catal. Lett.* **1997**, *45*, 85.
(7) Gsell, M.; Jakob, P.; Menzel, D. *Science* **1998**, *280*, 717.
(8) Larsen, J. H.; Chorkendorff, I. *Surf. Sci.* **1998**, *405*, 62.
(9) Mavrikakis, M.; Hammer, B.; Norskov, J. K. *Phys. Rev. Lett.* **1998**, *81*, 2819.
(10) Rodriguez, J. A.; Goodman, D. W. *Science* **1992**, *257*, 897.
(11) Kampshoff, E.; Hahn, E.; Kern, K. *Phys. Rev. Lett.* **1994**, *73*, 704.
(12) Sander, D.; Schmidthals, C.; Enders, A.; Kirschner, J. *Phys. Rev. B* **1998**, *57*, 1406.
(13) Kamper, K. P.; Schmitt, W.; Guntherodt, G.; Kuhlenbeck, H. *Phys. Rev. B* **1988**, *38*, 9451.
(14) Koziol, C.; Lilienkamp, G.; Bauer, E. *Phys. Rev. B* **1990**, *41*, 3364.
(15) Campbell, R. A.; Rodriguez, J. A.; Goodman, D. W. *Surf. Sci.* **1990**, *240*, 71.
(16) Schmidthals, C.; Sander, D.; Enders, A.; Kirschner, J. *Surf. Sci.* **1998**, *417*, 361.
(17) Schmidthals, C.; Sander, D.; Enders, A.; Kirschner, J. *Surf. Sci.* **1998**, *402−404*, 636.
(18) Whitten, J. E.; Gomer, R. *Surf. Sci.* **1994**, *316*, 23.
(19) Berlowitz, P. J.; Goodman, D. W. *Surf. Sci.* **1987**, *187*, 463.
(20) Khan, N. A.; Hwu, H. H.; Chen, J. G. *J. Catal.* **2002**, *205*, 259.
(21) Fruhberger, B.; Chen, J. G. *J. Am. Chem. Soc.* **1996**, *118*, 11599.
(22) Tamm, P. W.; Schmidt, L. D. *J. Chem. Phys.* **1971**, *54*, 4775.
(23) Hammer, B.; Norskov, J. K. *Adv. Catal.* **2000**, *45*, 71.
(24) Kitchin, J. R.; Barteau, M. A.; Chen, J. G. In preparation.
(25) Polizotti, B. D.; Hwu, H. H.; Chen, J. G. *Surf. Sci.* **2002**, *520*, 97.
(26) Chen, J. G. *Surf. Sci. Rep.* **1997**, *30*, 1.